SPACE TELESCOPE SCIENCE INSTITUTE
Operated for NASA by AURA

Instrument Science Report ACS 2004-04

Elevated temperature measurements of ACS charge transfer efficiency (CTE)

Max Mutchler and Adam Riess
March 1, 2004

ABSTRACT

On 6 March 2003, the ACS operating temperature was temporarily elevated from it's nominal set point of -77 C to study the effect on dark current (especially hot pixels) and charge transfer efficiency (CTE) in the CCDs. A companion report presents the hot pixel analysis (ACS Instrument Science Report 2003-04), while this report presents the CTE analysis. Together, these reports provide some insight into the possible effects of lowering the ACS operating temperature, possibly to -80 C or colder, if the Aft Shroud Cooling System is installed during Hubble Space Telescope (HST) Servicing Mission 4.

Introduction

The CCDs in the Advanced Camera for Surveys (ACS) have been operating at their lowest feasible temperature of -77 C since being installed in the *Hubble Space Telescope* (HST) in March 2002. On 6 March 2003, HST calibration program 9707 (PI Colin Cox) obtained typical dark and CTE frames at the nominal temperature, and also at two elevated temperatures, -71.5 C and -66.7 C.

This allows us to study the temperature dependence of two key CCD characteristics: the dark current (including the number of hot pixels) and the charge transfer efficiency (CTE). For a more complete description of the elevated temperature observations, and results of the dark current analysis, see *ACS Instrument Science Report 2003-04* by Cox et al. In this report, we present the CTE analysis.

CTE is a function of many interdependent factors: radiation dose (number of induced traps), trapping timescales, read-out speed, signal size, background signal, clocking waveform, number of transfers (size of the detector), and temperature. Therefore, different methods of measuring CTE often yield results which are different, or at least difficult to directly compare, because none of the methods fully isolate these underlying factors.

Program 9707 allowed for two independent but similar methods of measuring the CTE at elevated temperatures. All of the data was all collected at one point in time, so the radiation dose (i.e. number of charge traps) is a constant. Furthermore, both methods are based on recovering and measuring charge which has been trapped and released on very short timescales (within ~10 WFC charge transfers or ~32 milliseconds). Shockley-Hall-Reed Theory describes the charge release timescale as follows (Janesick, 2001):

$$\tau_e = \frac{e^{E_t / kT}}{\sigma v_{th} N_c}$$

where for each trap:

τ_e is the timescale for charge emission (de-trapping), σ is the cross section, E_t is the trapping state energy below the conduction band (for electron traps) and above the valence band (for hole traps), v_{th} is the thermal velocity of the carriers, and N_c is the effective density of states.

The short-timescale “deferred charge” manifests itself in two ways: as excess charge (above the bias level) in CCD overscans, and also as faint comet-like tails (which are preferentially aligned with the CCD readout direction) trailing bright source pixels.

In this report, we present an analysis of only the *parallel* CTE in the WFC chips. By design, CCD serial registers have much faster clocking, for efficient read outs. So the *serial* CTE is almost unmeasureably small under any circumstances, and any differences caused by varying the temperature are undiscernable from these tests. Some HRC dark frames were obtained by program 9707 (but no HRC EPER frames), but their analysis is not included here. The CTE problem is much less acute in the 1024 x 1024 pixel HRC chip, where charge packets undergo fewer transfers while being read out, than in the 4096 x 2048 pixel WFC chips.

Deferred charge in overscans: Extended Pixel Edge Response (EPER)

The EPER test involves only internal exposures, so the data can be obtained easily (during Earth occultations) and consistently over the entire life of the CCD, including pre-flight. EPER does not provide an absolute CTE measurement, or one which is readily applicable to science data (see Riess, 2003). However, EPER results from any epoch over the lifetime of the detector can be directly compared, to monitor the relative decline in CTE -- a result of cumulative exposure to the harsh radiation environment of space (Bebek, 2001).

In an ideal CCD, the pixel values in the overscan region would faithfully reflect the bias level. The EPER test is a measurement of any excess charge in the overscan, with the presumption that it is charge which was trapped during the the readout of the science array, and then released during subsequent overscans.

The EPER data are essentially flat-field frames with different filters and exposure times which generate a range of signal levels. Crossed filters are used to test the very lowest signal levels where CTE losses are greatest as a fraction of total flux. EPER frames have extra-large overscan regions to accomodate the growing deferred charge tail there. These super-sized overscan regions are not necessary during the early years in orbit, but they will be important in later years when the deferred charge tail might otherwise completely obscure the underlying bias level. Once the bias level is subtracted from the overscan, the remaining (deferred) charge is measured, and the CTE is inferred as follows (excerpted from Jones et al., 1999):

$$CTE(Q_o, n) = \left(1 - \frac{\Delta Q_n}{Q_o}\right)^{\frac{1}{n}}$$

Variables $\mathbf{Q_o}$ and $\Delta\mathbf{Q_n}$ represent the reference signal level and leading row (or column) charge deficit, respectively, after **n** transfers of the leading row (or column). The CTE versus signal curve is measured by varying the value of $\mathbf{Q_o}$. In the case of EPER, variable $\Delta\mathbf{Q_n}$ equals the total amount of deferred charge in the exponential tail after **n** transfers of the last row (or column) of the physical image.

In Figure 1, the inferred CTE, based on EPER data from program 9707, is plotted over a range of signal levels for three set point temperatures. Only the data taken at the highest temperature (diamonds) shows a significant and consistent (at all signal levels) difference from the nominal temperature data (squares). The CTE, as measured by EPER, appears to improve at the higher temperature.

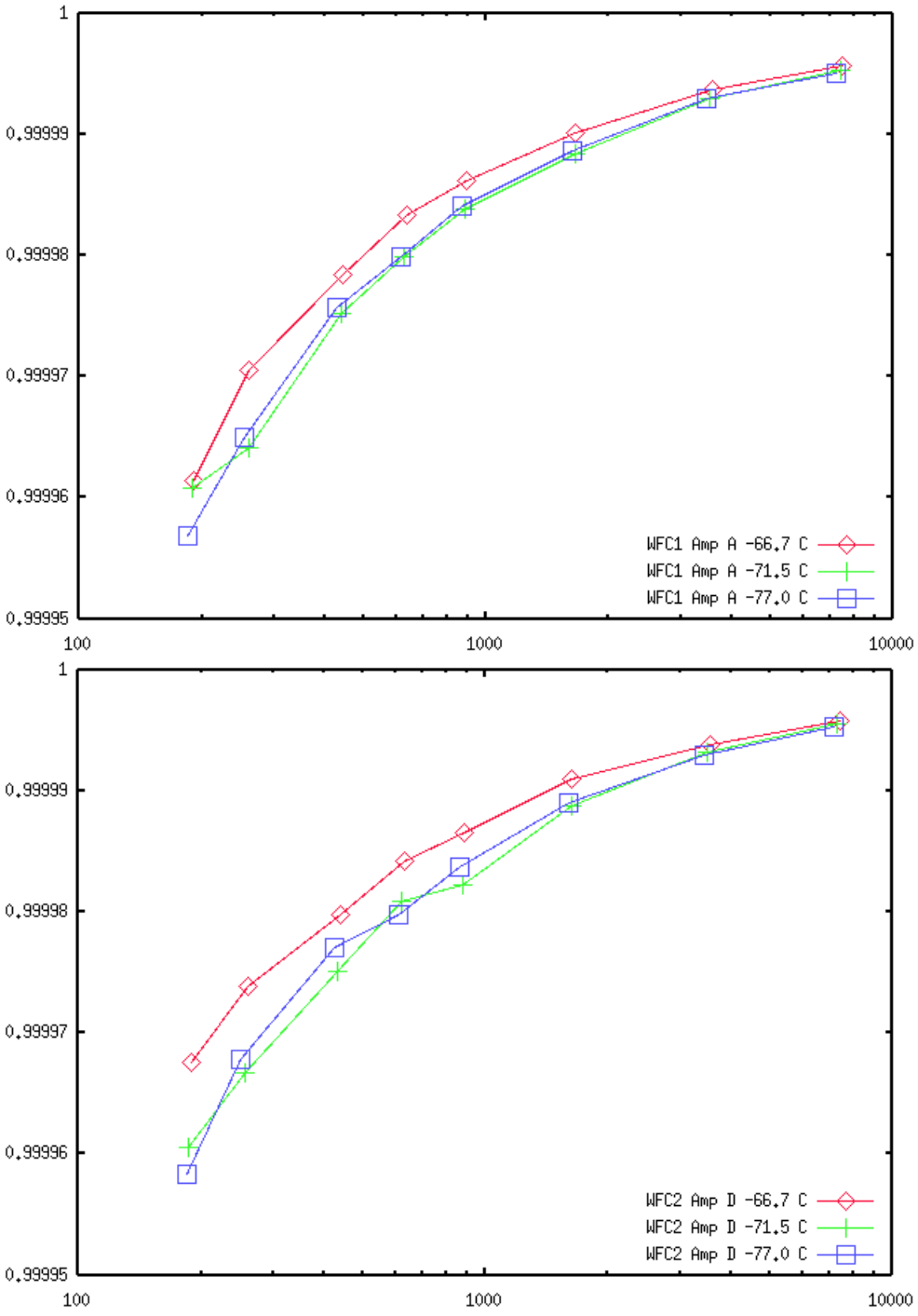

Figure 1: ACS parallel CTE per pixel versus signal level, for WFC chip 1 (upper) and chip 2 (lower), as inferred from EPER measurements on 6 March 2003. Measurements were made at the nominal operating temperature of -77.0 C (squares), at -71.5 C (crosses), and at -66.7 C (diamonds).

Figure 2 shows a profile of one of the overscans used to make an EPER measurement at the lowest signal level, where the CTE is most affected by charge traps. Note that at the higher temperature (-66.7 C), the *amplitude* of the deferred charge tail is actually higher than at the lower temperature, i.e. there is more deferred charge in the first overscan pixel. Although the amplitude is greater, the tail drops off more quickly, such that there is less *total* charge (from which the CTE is inferred) over all 75 overscan pixels .

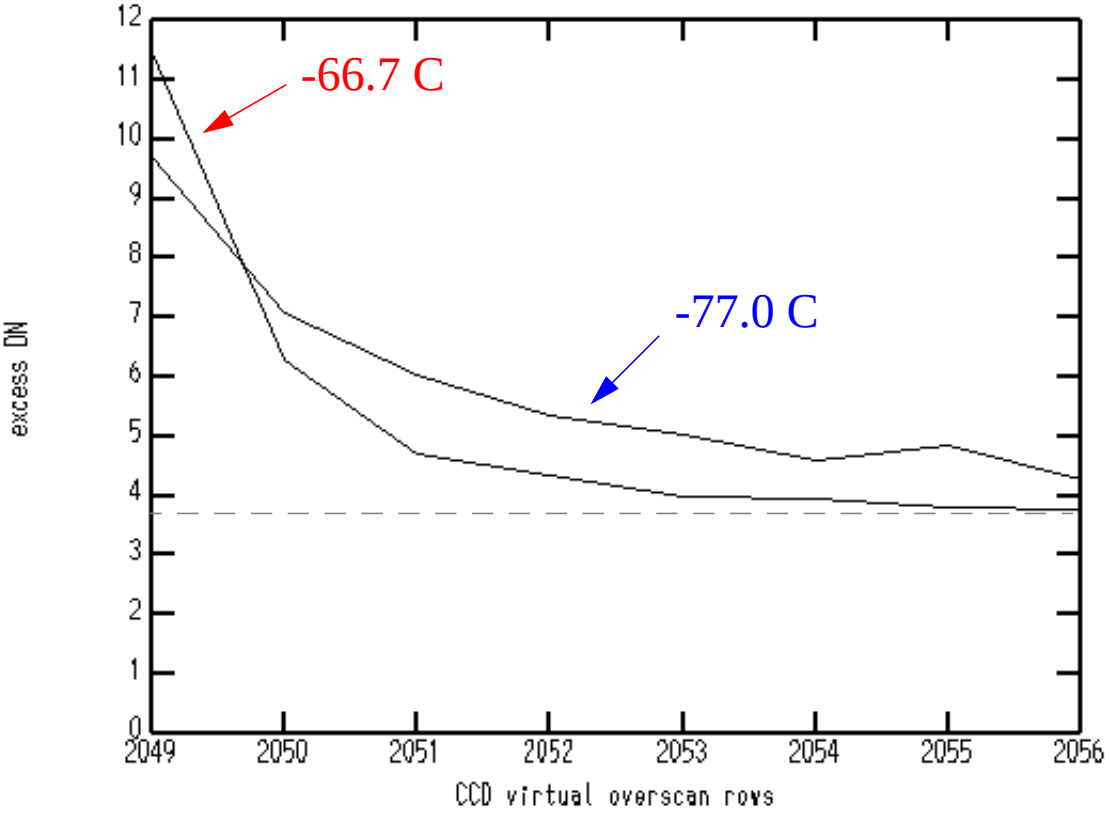

Figure 2: Sample profiles of ACS virtual overscans used to measure EPER at different temperatures. These are WFC chip 2 overscans for EPER data with the lowest signal (~185e) tested. Note that for chip 2, the (extra-large) virtual overscan is the last 75 rows (starting at row 2049), whereas for chip 1 it is the first 75 rows.

Deferred charge in the science array: hot pixel and cosmic ray tails

For both the WFC and HRC, three typical 1000-second dark frames were obtained at each of the three temperature set points in program 9707. The analysis of the dark current and hot pixels in these darks are provided in another report (Cox et al., 2003). These dark frames also contain many hot pixels and cosmic rays which exhibit faint tails in the anti-clocking direction, which are created by the short-timescale release of trapped charge. See Riess et al. (1999) for a detailed description of how these tails are used to measure CTE.

In Figure 3, the mean profiles of CTE tails in dark frames from program 9707 are plotted for the three set point temperatures. As the temperature increases, the tail amplitude increases, while the emission timescale (scale length) decreases -- as predicted by theory. The total charge also decreases at the higher temperature, which is analagous to (and in agreement with) the EPER measurements described above. Also note that for a given photometric aperture, a smaller amount of charge is lost (i.e. deferred outside of the aperture) at higher temperatures. In Figure 4, these trends are further illustrated, and extrapolated towards colder temperatures.

If all the lost charge was deposited locally, i.e., in the tail, then our results would predict less net loss at higher temperatures in a fixed aperture because the tail becomes shorter and less charge is lost outside the aperture. Likewise, we would expect less net loss for a larger aperture at fixed temperature because, again, less charge is lost outside the aperture.

However, we do not see less loss with larger aperture because the local charge in the tail accounts for only a small fraction (2-3%) of the total charge lost by a source (i.e., the deferred charge tail is only the tip of the iceberg).

Similar results from WFPC2

Shortly after HST Servicing Mission 3A in December 1999, dark frames were obtained during the CCD cooldown program (SMOV program 8941, see Casertano et al, 2000) of the Wide Field Planetary Camera 2 (WFPC2).

The analysis of CTE tails in these WFPC2 dark frames (Riess, 2000) shows that they exhibit the same dependence on temperature as their ACS counterparts. In Figure 5, the amplitude of the WFPC2 CTE tails are greater at - 55C, but they decline faster than at -88 C.

Furthermore, an earlier reduction in the WFPC2 operating temperature, during it’s initial Orbital Verification in 1994, led to less overall photometric CTE loss in the WFPC2 CCDs (Holtzman, et al., 1995)

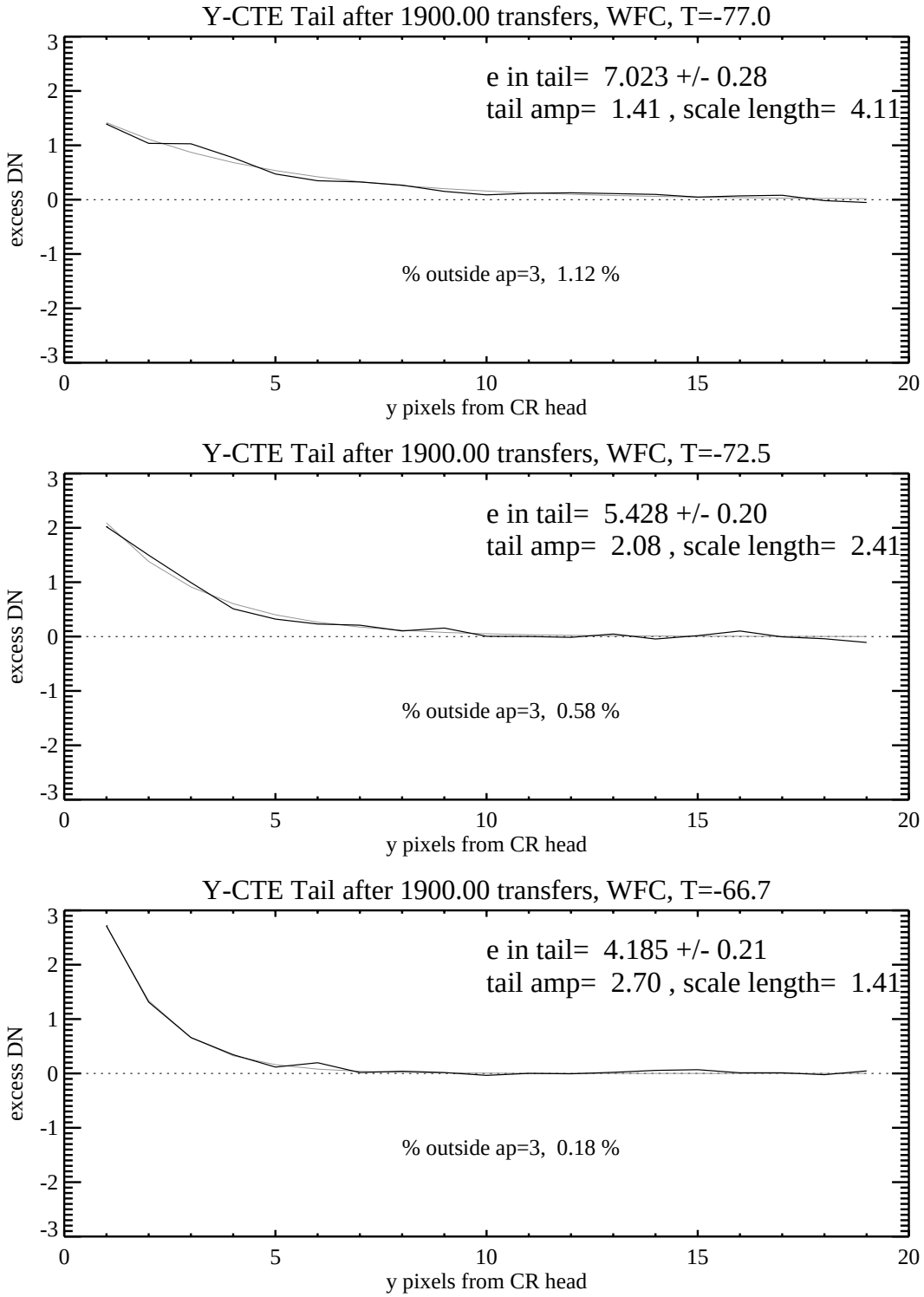

Figure 3: Mean characteristics of deferred charge tails of hot pixels in ACS/WFC dark frames taken at three temperatures. The normal CCD operating temperature is -77 C (top).

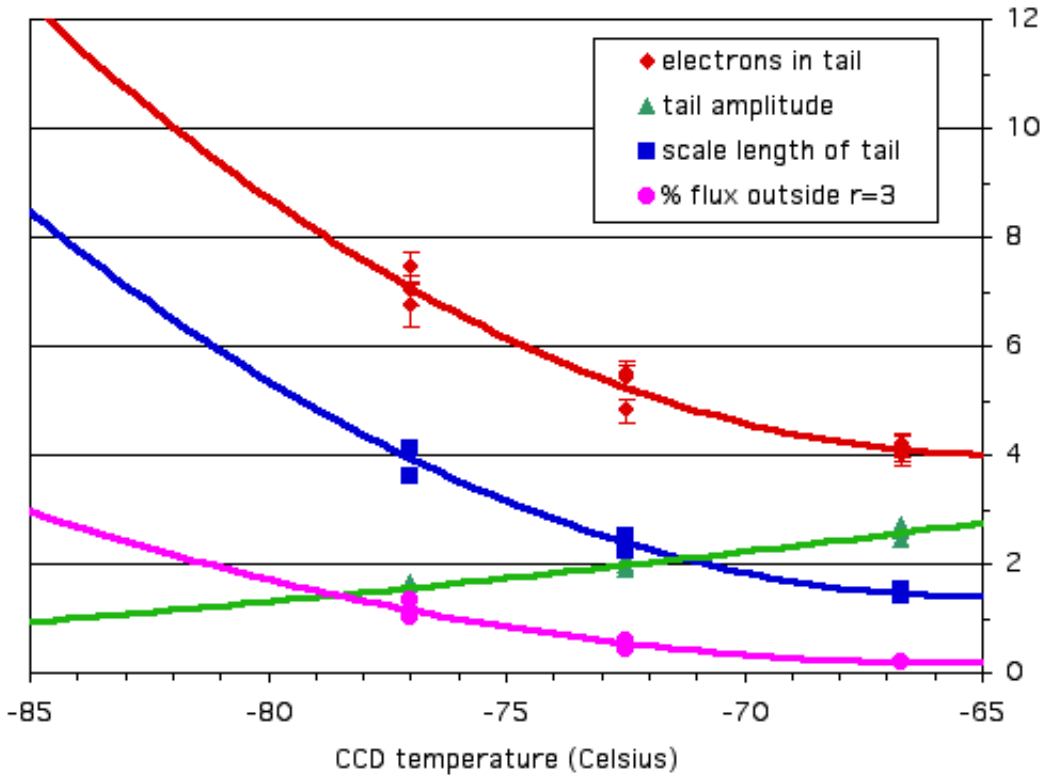

Figure 4: ACS/WFC hot pixel tail characteristcs as a function of temperature. The measurements (points) are fitted with simple polynomials. The tail amplitude increases at higher temperatures, while the scale length and total charge decreases. The flux lost (as a percentage of the original pixel flux) outside of an aperture r=3 decreases at higher temperatures.

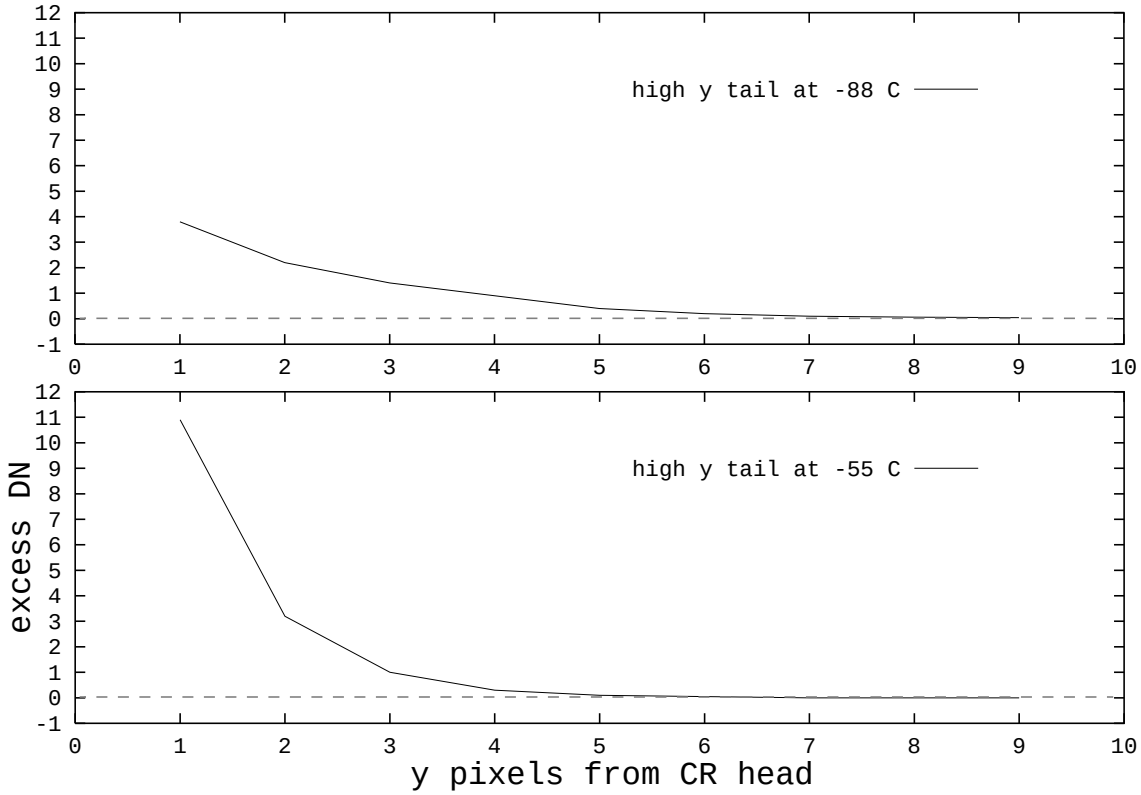

Figure 5: Results of a similar WFPC2 test in 2000 (Riess, private notes), using darks taken during the post-SM3A CCD cooldown (SMOV program 8941). A comparison of hot pixel tails in darks taken at the nominal operating temperature of -88 C (top), and the elevated temperature of -55 C (bottom) for pixels which are many parallel transfers away from the readout register (high y), and pixels which are near the readout register (low y, or very few parallel transfers).

Analysis and Conclusions

Both of the ACS elevated temperature CTE tests presented here show a decrease of *total* deferred charge at higher temperatures. At first glance, this would seem to indicate that CTE might improve at higher temperatures, and by extrapolation, be worse (or at least unpredictable) at lower temperatures.

But we know the short-timescale deferred charge, which our tests have measured, is only a small fraction of the net deferred charge. Earlier reports have characterized the long-timescale release of trapped charge in the WFPC2 CCDs (Biretta & Mutchler, 1997, Biretta & Platais, 2004 - in preparation), and shown that most of the trapped charge (over 90%) is released on timescales of minutes, rather than milliseconds. All trapped charge, regardless of it's release timescale, contributes to the total CTE loss.

So how can we use the temperature dependence of short-timescale deferred charge to infer the temperature dependence of the total lost charge? From WFPC2 we saw that the temperature dependence of the total photometric loss was anti-correlated with the temperature dependence of the deferred charge (though positively correlated with the amplitude of the deferred charge tail). Assuming the same relation between short and long timescale charge trapping holds for ACS as for WFPC2 (i.e., that the distribution of trap depths is similar), we would expect less loss and better CTE at lower temperatures.

The earlier WFPC2 results imply that, although we see more total deferred charge at lower temperatures on short timescales, for ACS we may still expect the overall CTE to improve at lower temperatures, e.g. -85 C or -90 C (Johnson, 1998), if the Aft Shroud Cooling System (Cox & Cottingham, 2001) is installed during Hubble Servicing Mission 4. Unfortunately, our limited dataset is inadequate for quantifying precisely how much better, but we would expect the ACS CCDs to behave like the WFPC2 CCDs in this regard.

Acknowledgements

We thank Marco Sirianni and Colin Cox for their contributions to this report.

References

Bebek, et al, 2001, “Proton Radiation Damage in P-Channel CCDs Fabricated on High-Resistivity Silicon”, IEEE
http://snap.lbl.gov/pubdocs/CCDpaper_rev2.pdf

Biretta & Platais, 2004, “Hot Pixels as a Probe of CTE effects”, WFPC2 Instrument Science Report (in preparation)

Biretta & Mutchler, 1997, “Charge Trapping and CTE Residual Images in the WFPC2 CCDs”, WFPC2 Instrument Science Report 1997-05
http://www.stsci.edu/instruments/wfpc2/Wfpc2_isr/wfpc2_isr9705.html

Casertano et al., 2000, “Results of the WFPC2 Observatory Verification after Servicing Mission 3A”, WFPC2 Instrument Science Report 2000-02
http://www.stsci.edu/instruments/wfpc2/Wfpc2_isr/wfpc2_isr0002.html

Cox, Mutchler, Van Orsow, 2003, “Elevated temperature measurements of hot pixels”,
ACS Instrument Science Report 2003-04:
http://hst.stsci.edu/acs/documents/isrs/isr0304.pdf

Cox & Cottingham, 2001, “ACS Thermal Control With ASCS”,
ACS Instrument Science Report 2001-05:
http://hst.stsci.edu/acs/documents/isrs/isr0105.pdf

Holtzman, et al., 1995, “The Photometric Performance and Calibration of WFPC2”, PASP v.107, p.1065

Janesick, J., 2001, Scientific Charge-Coupled Devices, SPIE Press

Johnson, G., 1998, “CCD operation at -90 C”,
ACS Ball Aerospace System Engineering Report THM-029

Jones, Clampin, Meurer, Schrein, 1999, “Justification and Requirements for On-Board ACS FPR/EPER CTE Calibration”, ACS Technical Instrument Report 1999-03
http://www.stsci.edu/hst/acs/documents/tirs/tir9903.pdf

Riess, A., 2003, “On-orbit calibration of ACS CTE corrections for photometry”,
ACS Instrument Science Report 2003-09:
http://hst.stsci.edu/acs/documents/isrs/isr0309.pdf

Riess, Biretta, Casertano, 1999, “Time Dependence of CTE from Cosmic Ray Trails”,
WFPC2 Instrument Science Report 1999-04:
http://www.stsci.edu/instruments/wfpc2/Wfpc2_isr/wfpc2_isr9904.html

Riess, 2000, private notes, based on data from HST/WFPC2 program 8941